Retromer Is Required for Apoptotic Cell Clearance by Phagocytic Receptor Recycling

Didi Chen, *et al.*

Science **327**, 1261 (2010);
DOI: 10.1126/science.1184840

4. J. Overmann, F. Garcia-Pichel, in *The Prokaryotes*, vol. 2, *Ecophysiology and Biochemistry*, M. Dworkin *et al.*, Eds. (Springer, New York, 2006), pp. 32–85.
5. C. V. Iancu *et al.*, *J. Mol. Biol.* **372**, 764 (2007).
6. M. F. Schmid *et al.*, *J. Mol. Biol.* **364**, 526 (2006).
7. C. A. Kerfeld *et al.*, *Science* **309**, 936 (2005).
8. S. Tanaka *et al.*, *Science* **319**, 1083 (2008).
9. H. Ohkawa, M. Sonoda, H. Katoh, T. Ogawa, *Can. J. Bot.* **76**, 1035 (1998).
10. G. D. Price, S. M. Howitt, K. Harrison, M. R. Badger, *J. Bacteriol.* **175**, 2871 (1993).
11. Materials and methods are available as supporting material on *Science* Online.
12. M. B. Elowitz, M. G. Surette, P. E. Wolf, J. B. Stock, S. Leibler, *J. Bacteriol.* **181**, 197 (1999).
13. T. E. Jensen, R. P. Ayala, *Arch. Microbiol.* **111**, 1 (1976).
14. C. V. Iancu *et al.*, *J. Mol. Biol.* **396**, 105 (2010).
15. M. Thanbichler, L. Shapiro, *Nat. Rev. Microbiol.* **6**, 28 (2008).
16. G. Ebersbach, K. Gerdes, *Annu. Rev. Genet.* **39**, 453 (2005).
17. N. Rosenfeld, J. W. Young, U. Alon, P. S. Swain, M. B. Elowitz, *Science* **307**, 1962 (2005).
18. A. Komeili, *Annu. Rev. Biochem.* **76**, 351 (2007).
19. H. J. Defeu Soufo, P. L. Graumann, *BMC Cell Biol.* **6**, 10 (2005).
20. S. R. Thompson, G. H. Wadhams, J. P. Armitage, *Proc. Natl. Acad. Sci. U.S.A.* **103**, 8209 (2006).
23. We thank R. Milo, R. Ward, R. Losick, S. Stanley, and E. Garner for comments on the manuscript; M. Ericsson and L. Benecchi for electron microscopy; and S. Golden for reagents. D.F.S. is a U.S. Department of Energy Biosciences Fellow of the Life Sciences Research Foundation. B.A. is supported by the Fundação para a Ciência e a Tecnologia and Graduate Program in Areas of Basic and Applied Biology (GABBA). This work was supported by Army Research Office Award W911NF-09-1-0226.

Supporting Online Material

www.sciencemag.org/cgi/content/full/327/5970/1258/DC1
Materials and Methods
SOM Text
Figs. S1 to S4
Tables S1 to S3
References
Movies S1 to S5

17 December 2009; accepted 22 January 2010
10.1126/science.1186090

Retromer Is Required for Apoptotic Cell Clearance by Phagocytic Receptor Recycling

Didi Chen,[1,2*] Hui Xiao,[1,2*] Kai Zhang,[3] Bin Wang,[3] Zhiyang Gao,[1] Youli Jian,[1] Xiaying Qi,[1] Jianwei Sun,[1,2] Long Miao,[3] Chonglin Yang[1†]

The cell surface receptor CED-1 mediates apoptotic cell recognition by phagocytic cells, enabling cell corpse clearance in *Caenorhabditis elegans*. Here, we found that the *C. elegans* intracellular protein sorting complex, retromer, was required for cell corpse clearance by mediating the recycling of CED-1. Retromer was recruited to the surfaces of phagosomes containing cell corpses, and its loss of function caused defective cell corpse removal. The retromer probably acted through direct interaction with CED-1 in the cell corpse recognition pathway. In the absence of retromer function, CED-1 associated with lysosomes and failed to recycle from phagosomes and cytosol to the plasma membrane. Thus, retromer is an essential mediator of apoptotic cell clearance by regulating phagocytic receptor(s) during cell corpse engulfment.

In *Caenorhabditis elegans*, cell corpse engulfment is controlled by two parallel pathways, one that recognizes and transduces engulfing signals, and the other that induces cytoskeleton reorganization (*1*). However, how components of these pathways are regulated and what other factors are involved remain unclear. To identify additional regulators of these pathways we performed genome-wide and candidate-based RNA interference (RNAi) screens (*2*) for genes whose inactivation greatly increased cell corpse numbers in the *C. elegans* germ line. Three genes, *snx-1*, *snx-6*, and *lst-4*, encoding homologs of mammalian sorting nexins 1/2, 5/6, and 9/18/33, respectively, were identified (figs. S1A and S2A and table S1). In mammals, sorting nexins 1/2 and 5/6 are essential components of the intracellular protein sorting complex retromer (*3*–*5*), whereas sorting nexins 9/18/33 regulate endocytosis (*3*). The deletion mutants *snx-1*(*tm847*) (*6*) and *snx-*

[1]Key Laboratory of Molecular and Developmental Biology, Institute of Genetics and Developmental Biology, Chinese Academy of Sciences, Datun Road, Chaoyang District, Beijing 100101, China. [2]Graduate School, Chinese Academy of Sciences, Beijing 100039, China. [3]National Laboratory of Biomacromolecules, Institute of Biophysics, Chinese Academy of Sciences, Datun Road, Chaoyang District, Beijing 100101, China.

*These authors contributed equally to this work.
†To whom correspondence should be addressed. E-mail: clyang@genetics.ac.cn

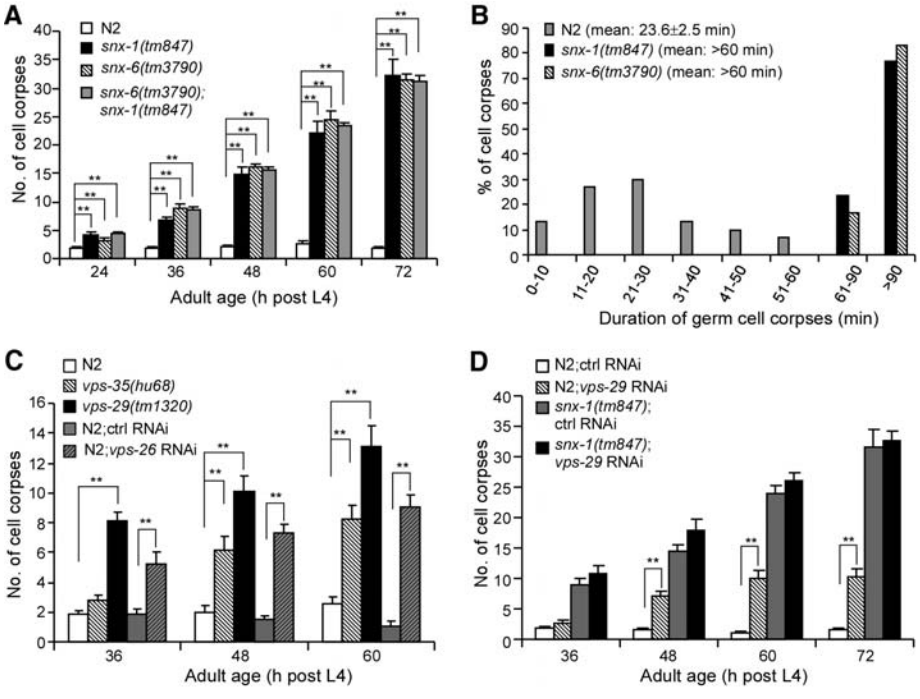

Fig. 1. *C. elegans* retromer affects clearance of apoptotic cells. (**A**) Quantification of germ cell corpses in N2 (wild type), *snx-1*(*tm847*), *snx-6*(*tm3790*), and *snx-6*(*tm3790*);*snx-1*(*tm847*) mutants. (**B**) Four-dimensional microscopy analysis of germ cell corpse duration in N2, *snx-1*(*tm847*), and *snx-6*(*tm3790*) mutants. Thirty germ cell corpses were recorded for each strain. (**C**) Quantification of germ cell corpses in *vps-26*(*RNAi*), *vps-35*(*hu68*), and *vps-29*(*tm1320*) animals. (**D**) Germ cell corpse phenotypes of control RNAi- and *vps-29* RNAi-treated N2 and *snx-1*(*tm847*) mutants. In (A), (C), and (D), the *y* axis indicates the average number of germ cell corpses. Error bars represent the SEM. Comparisons were performed using unpaired *t* tests. $^{**}P < 0.001$.

6(*tm3790*), which probably represent strong loss-of-function mutations of *snx-1* and *snx-6* (figs. S1B and S2B), had increased numbers of germline and embryonic cell corpses, which persisted significantly longer than did the wild type (Fig. 1, A and B, and fig. S3). The number of cell deaths in *snx-1*(*tm847*) and *snx-6*(*tm3790*) embryos was indistinguishable from that of the wild type; thus, the increased cell corpse numbers result from defective corpse clearance rather than excessive apoptosis.

The retromer mediates retrograde transport of transmembrane cargoes from endosomes to the trans-Golgi network (*4*). SNX-1 and SNX-6 are essential subunits of the retromer sorting nexin dimer (*4*, *5*). In *snx-6*(*tm3790*);*snx-1*(*tm847*) double mutants, germline and embryonic cell corpse numbers were indistinguishable from those of single mutants (Fig. 1A and fig. S3A), suggesting that these genes function in the same genetic pathway. In contrast, *lst-4*(*tm2423*);*snx-1*(*tm847*) double mutants exhibited significantly more germline and embryonic cell corpses than did single mutants (fig. S4). Thus, LST-4 probably acts separately from the retromer during cell corpse clearance. The retromer also contains a Vps26-Vps29-Vps35 trimer (*4*), so we examined *vps-26*(*tm1523*), *vps-29*(*tm1320*), and *vps-35*(*hu68*) deletion mutants (*6*). No corpse phenotype was observed in *vps-26*(*tm1523*) germ lines, probably because of abnormal germline development (*6*, *7*). Partial RNAi inactivation of *vps-26*, however, significantly increased germ cell corpses (Fig. 1C). A similar increase was observed in *vps-29*(*tm1320*) and *vps-35*(*hu68*) germ lines (Fig. 1C). Intriguingly, cell corpse numbers in *vps-26*(*tm1523*), *vps-29*(*tm1320*), and *vps-35*(*hu68*) embryos were similar to those of the wild type. Thus, loss of individual retromer components affects corpse clearance to different extents. We next asked whether the VPS-26–VPS-29–VPS-35 and sorting nexin subcomplexes acted together in cell corpse removal. *vps-29* RNAi on its own caused an increase in germ cell corpses, but did not further enhance the number of corpses in *snx-1*(*tm847*) germ lines (Fig. 1D), suggesting that *snx-1* and *vps-29* probably function in the same genetic pathway. Furthermore, in glutathione-*S*-transferase (GST) pull-down assays, SNX-1 and SNX-6 interacted with one another, and with GST-VPS-26, -29, and -35 (fig. S5). Thus, retromer components function together during cell corpse clearance in *C. elegans*.

We next examined germ cell corpse engulfment by transmission electron microscopy. In wild-type animals treated with *gla-3* RNAi, which increases germ cell deaths without affecting corpse clearance (*8*), 10 cell corpses from 4 gonad arms were fully encircled by gonadal sheath cells (Fig. 2), consistent with previous findings that wild-type germ cell corpses are swiftly engulfed (*9*). Of 31 cell corpses from 2 gonad arms in *snx-1*(*tm847*) mutants, 25 (81%) were only partially encircled by sheath cells, while 6 (19%) were completely engulfed but not properly degraded [Fig. 2, fig. S6, and supporting online material (SOM) text]. Furthermore, engulfing cells required SNX-1/retromer activity for cell corpse removal, and SNX-1 and VPS-29 were recruited and colocalized on the cell corpse surface (SOM text and figs. S7 and S8). Thus, SNX-1/retromer is required for engulfment and degradation of cell corpses.

To determine in which pathway retromer acted, we examined double mutants of *snx-1*(*tm847*) with strong loss-of-function alleles of engulfment genes. In *C. elegans*, *ced-1*, *ced-6* (GULP), *ced-7* (ABC transporter), and *dyn-1* (Dynamin) function in one pathway to recognize and transduce engulfing signals, whereas *ced-2* (CrkII), *ced-5* (Dock 180), *ced-10* (Rac guanosine triphosphatase), *ced-12* (ELMO), and *psr-1* (phosphatidylserine receptor) act in the other pathway to activate cytoskeleton rearrangement (*1*, *10*). Germline and embryonic cell corpse numbers in double mutants of *snx-1*(*tm847*) with *ced-1*(*e1735*) or *ced-6*(*n2095*) were indistinguishable from those of *ced-1*(*e1735*) and *ced-6*(*n2095*) single mutants (Fig. 2G and fig. S9, A to C). Intriguingly, both germline and embryonic cell corpses in *ced-7*(*n1892*);*snx-1*(*tm847*) double mutants were significantly increased compared to *ced-7*(*n1892*) single mutants (Fig. 2H and fig. S9D). Thus, *snx-1*/retromer probably acts in parallel to *ced-7* in the same pathway as *ced-1* and *ced-6*. Consistent with this, *snx-1*(*tm847*) significantly enhanced germline and embryonic cell corpse numbers in mutants affecting the other engulfment pathway (Fig. 2, I and J, and fig. S9, E to H).

During phagocytosis, the receptor CED-1 clusters in the phagocytic cup before quickly

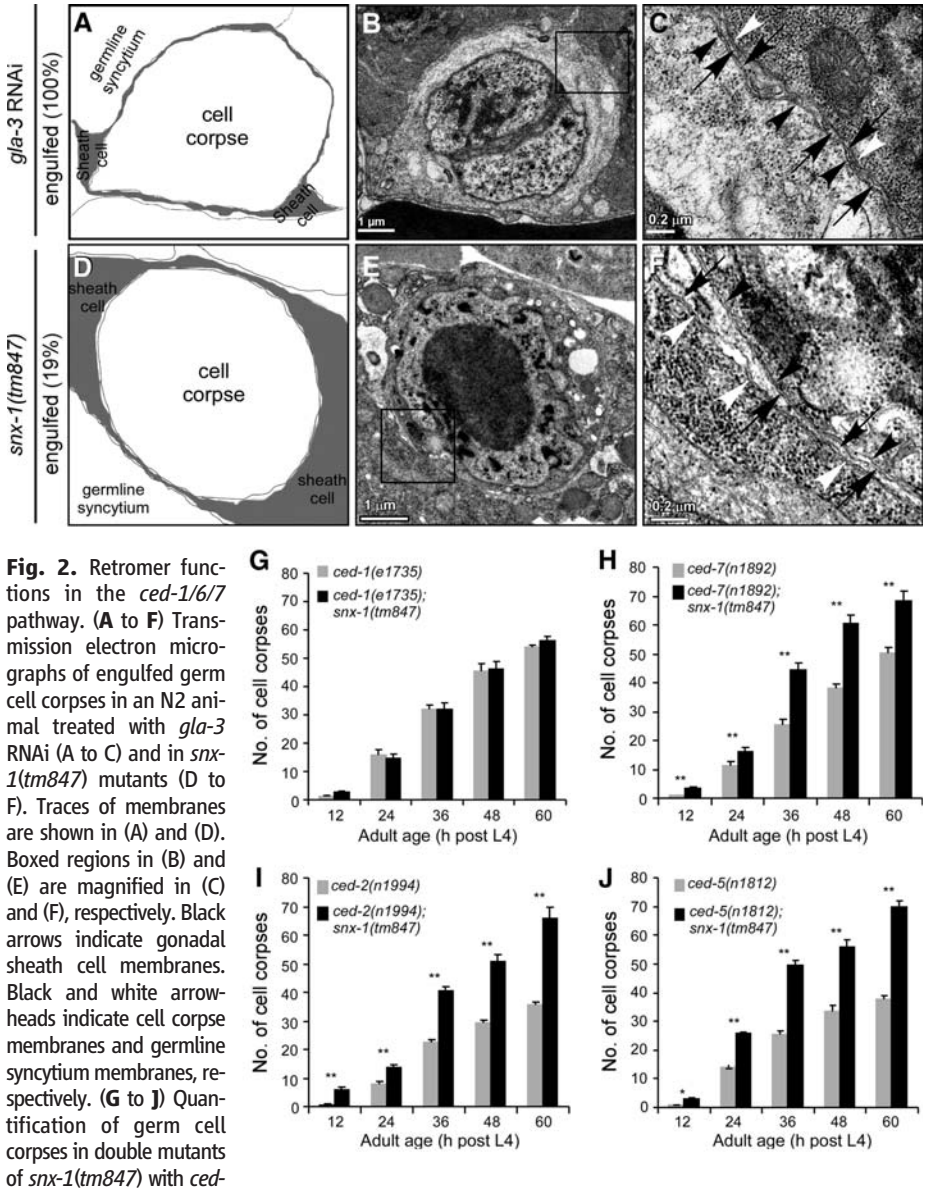

Fig. 2. Retromer functions in the *ced-1/6/7* pathway. (**A** to **F**) Transmission electron micrographs of engulfed germ cell corpses in an N2 animal treated with *gla-3* RNAi (A to C) and in *snx-1*(*tm847*) mutants (D to F). Traces of membranes are shown in (A) and (D). Boxed regions in (B) and (E) are magnified in (C) and (F), respectively. Black arrows indicate gonadal sheath cell membranes. Black and white arrowheads indicate cell corpse membranes and germline syncytium membranes, respectively. (**G** to **J**) Quantification of germ cell corpses in double mutants of *snx-1*(*tm847*) with *ced-1*(*e1735*) (G), *ced-7*(*n1892*) (H), *ced-2*(*n1994*) (I), and *ced-5*(*n1812*) (J) mutants. Data derived from two different genetic backgrounds at multiple stages were compared by unpaired *t* tests. $*P < 0.05$, $**P < 0.001$.

encircling the cell corpse. Recognition of apoptotic cells by CED-1 requires CED-7, loss of which disrupts clustering of CED-1 around embryonic cell corpses (*11*). Because retromer and CED-7 act in parallel in the *ced-1* pathway, we investigated whether retromer regulates CED-1 by time-lapse chasing the association of CED-1::GFP (green fluorescent protein) expressed from an integrated array (*smIs34*) with cell corpses in *snx-1*(*tm847*) embryos, while simultaneously monitoring phagosomal recruitment of lysosomes labeled by the lysosome marker LMP-1::mCherry. In wild-type embryos, CED-1::GFP was quickly recruited to the phagocytic cup and encircled the cell corpse within 3 min (Fig. 3A). Between 3 and 9 min, CED-1 disappeared from the phagosome and reappeared on the plasma membrane of the engulfing cell. As the CED-1 ring formed, lysosomes were simultaneously recruited to the phagosome as indicated by formation of a LMP-1::mCherry ring, which remained associated with the phagosome after CED-1 was released (Fig. 3A). Thus, CED-1 is recycled swiftly from the phagosome to the engulfing cell membrane before the cell corpse is degraded. The mean duration of the CED-1 ring on the phagosome was 10.8 ±1.7 min (n = 6) in wild-type embryos, but in *snx-1*(*tm847*);*smIs34* embryos it was 26.0 ± 1.8 min (n = 6) so that the ring remained associated with the phagolysosome until late in corpse degradation (Fig. 3A). Subsequently, when the corpses had adopted a pit-like structure, the proportion colabeled with CED-1::GFP and LMP-1::mCherry was <20% in wild-type embryos but >80% in *snx-1*(*tm847*) embryos (Fig. 3B). Thus, loss of retromer inhibits CED-1 recycling from the phagosome to the engulfing cell membrane, and phagosome-associated CED-1 is sent to lysosomes together with cell corpses. Furthermore, whereas *smIs34*-expressed CED-1::GFP was almost exclusively associated with the plasma membrane in wild-type embryos, in *snx-1*(*tm847*) embryos it displayed an intracellular punctate distribution pattern that colocalized with LMP-1::mCherry in addition to its membrane localization in several cell types such as hypodermal cells (Fig. 3C). Thus, CED-1 is internalized from and recycled back to the cell membrane; loss of retromer function causes lysosomal accumulation of CED-1. Consistent with this, CED-1::GFP expression driven by the *vps-33* promoter in macrophage-like coelomocytes was intracellular and partially overlapped with the lysosome marker mCherry::CUP-5 in *snx-1*(*tm847*) and *snx-6*(*tm3790*) mutants, whereas in the wild type it was mainly seen on the plasma membrane (SOM text and fig. S10A).

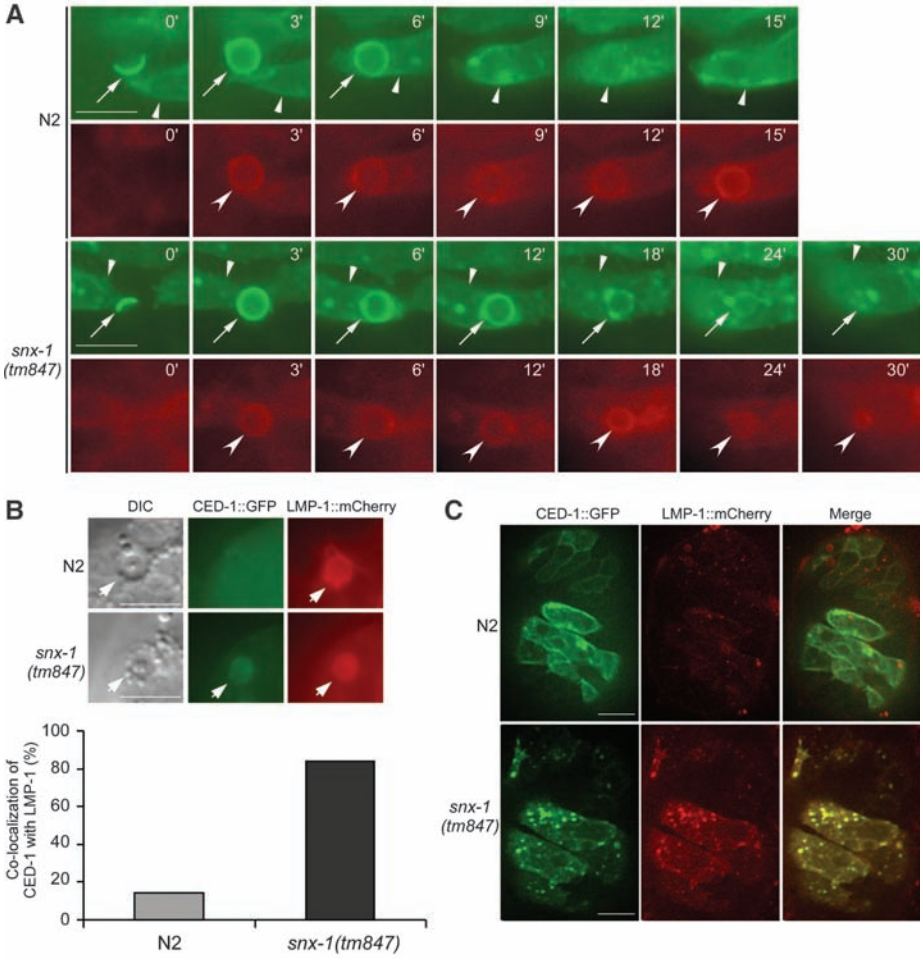

Fig. 3. *snx-1*(*tm847*) causes defective recycling of internalized CED-1. (**A**) Time-lapse chasing of CED-1::GFP (arrows) and LMP-1::mCherry (sharp arrowheads) on phagosomes in N2 and *snx-1*(*tm847*) animals. Clustering of CED-1::GFP on the phagocytic cup was set as 0 min. Blunt arrowheads indicate membranes of engulfing cells. Bars, 5 μm. (**B**) Representative images (top) and quantification (bottom) of CED-1::GFP and LMP-1::mCherry colocalization on cell corpses at a late stage of degradation in N2 and *snx-1*(*tm847*) embryos. At least 100 cell corpses in each strain were examined. Arrows indicate cell corpses. DIC, differential interference contrast. Bars, 5 μm. (**C**) Localization of CED-1::GFP and LMP-1::mCherry in hypodermal cells in N2 and *snx-1*(*tm847*) embryos. Bars, 10 μm.

The increased association of CED-1 with lysosomes suggests that CED-1 undergoes lysosome-mediated degradation. CED-1::GFP signal from *smIs34* was reduced in *snx-1*(*tm847*) mutants compared to the wild type (fig. S10B). CED-1::GFP protein abundance was significantly lower in *snx-1*(*tm847*);*smIs34* and *snx-6*(*tm3790*);*smIs34* animals (Fig. 4A). CED-1::GFP was also reduced in *vps-29*(*tm1320*);*smIs34* worms, though to a lesser extent. In contrast, CED-1::GFP was not reduced in *lst-4*(*tm2423*);*smIs34* animals (Fig. 4A). Using a CED-1 C-terminal–specific antibody, we found that endogenous CED-1 was strongly reduced in *snx-1*(*tm847*) and *snx-6*(*tm3790*) animals, slightly reduced in *vps-29*(*tm1320*) mutants, and undetectable in *ced-1*(*e1735*) mutants containing an early stop codon in the *ced-1* gene (Fig. 4B). Furthermore, endogenous CED-1 localized to the plasma membrane in wild-type embryos but not in *snx-1*(*tm847*) or *ced-1*(*e1735*) mutants (Fig. 4C). Thus, in the absence of retromer function, CED-1 fails to localize to the plasma membrane and is probably degraded in lysosomes, becoming limiting for cell corpse engulfment and causing accumulation of cell corpses. Consistent with this, RNAi knockdown of *vps-37*, a component of the ESCRT-I complex (endosomal sorting complex required for transport) (*12*), partially restored CED-1::GFP abundance in *snx-1*(*tm847*);*smIs34* animals (fig. S11). Moreover, the increased germline and embryonic corpse numbers in *snx-1*(*tm847*) mutants were strongly reduced by overexpressing CED-1::GFP driven by the *ced-1* promoter (*smIs34*) (Fig. 4D and fig. S12A). CED-1::GFP driven by the sheath cell-specific *lim-7* promoter (*bcIs39*) similarly decreased the number of *snx-1*(*tm847*) germline corpses (Fig. 4D). Furthermore, *smIs34* greatly reduced the numbers of both embryonic and germline cell corpses in *snx-6*(*tm3790*) single mutants as well as in *snx-6*(*tm3790*);*snx-1*(*tm847*) double mutants, but not in *lst-4*(*tm2423*) mutants (fig. S12, B to G), indicating that CED-1 overexpression specifically rescued the cell corpse phenotypes of retromer mutants and that retromer acts through CED-1 to affect cell corpse clearance.

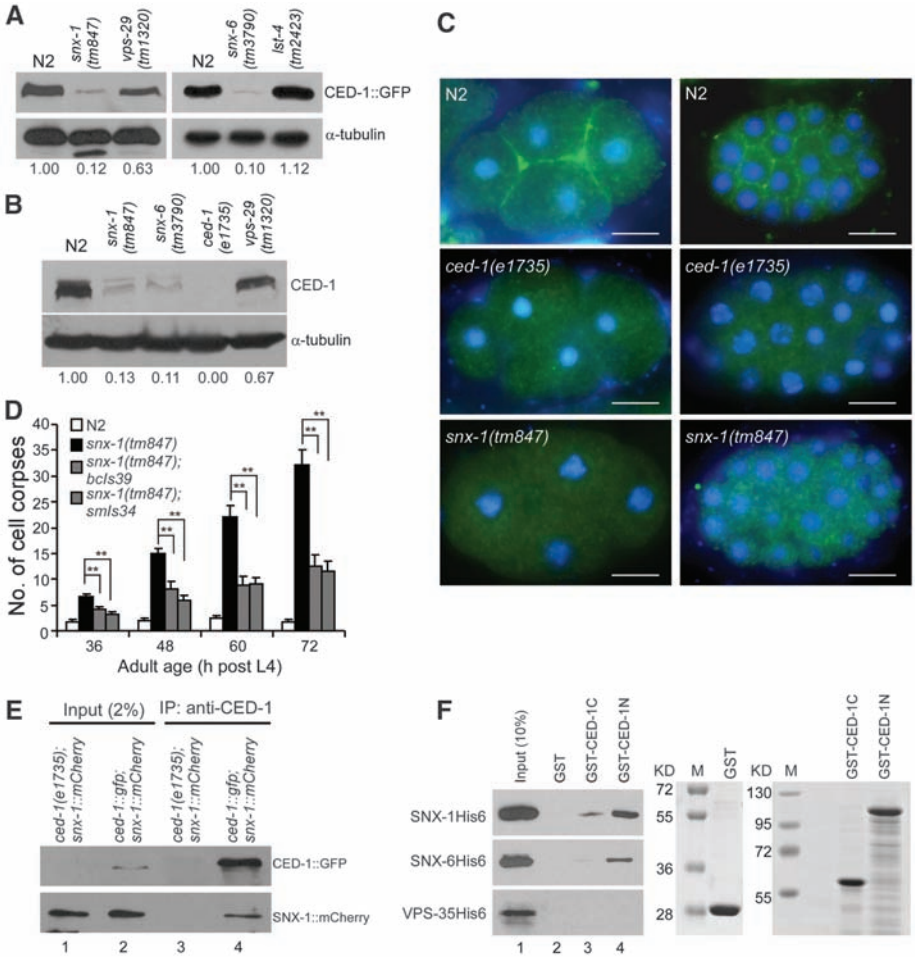

Fig. 4. Retromer acts through CED-1. (**A** and **B**) Immunoblot analysis of CED-1::GFP expression by *smIs34* ($P_{ced\text{-}1}$*ced-1::gfp*) (A) and endogenous CED-1 protein abundance (B) in N2 and different mutants. The relative expression of CED-1 in each strain is indicated. (**C**) Localization of endogenous CED-1 in N2, *ced-1*(*e1735*), and *snx-1*(*tm847*) embryos. Merged images of CED-1–specific antibody staining (green) and nuclear staining (blue) of a four-cell-stage embryo (left) and a ~50-cell-stage embryo (right) are shown. Bars, 10 μm. (**D**) Quantification of germ cell corpses in N2, *snx-1*(*tm847*), *snx-1*(*tm847*);*smIs34*, and *snx-1*(*tm847*);*bcIs39* ($P_{lim\text{-}7}$*ced-1::gfp*) animals. $^{**}P < 0.001$. (**E**) Immunoprecipitations (IP) were performed with CED-1–specific antibody from lysates of *ced-1*(*e1735*) mutants expressing SNX-1::mCherry (lane 1) and N2 worms expressing both CED-1::GFP and SNX-1::mCherry (lane 2). Proteins were detected with antibodies against GFP and mCherry, respectively. (**F**) His6-tagged SNX-1, SNX-6, and VPS-35 were incubated with immobilized GST, GST-CED-1C, and GST-CED-1N. Bound proteins were detected with antibody to His6 (left). GST fusion proteins used for binding are shown on the right.

Finally, using the CED-1 C-terminal–specific antibody, we immunoprecipitated CED-1::GFP from cell lysates from wild-type animals expressing both CED-1::GFP and SNX-1::mCherry and found that SNX-1::mCherry was associated with CED-1::GFP, whereas no SNX-1::mCherry was coimmunoprecipitated from lysates of *ced-1*(*e1735*) worms expressing SNX-1::mCherry alone (Fig. 4E). Thus, CED-1 associates with retromer in *C. elegans*. In a pull-down assay, purified SNX-1 interacted with GST-fused CED-1 N terminus (CED-1N, amino acids 1 to 908) and C terminus (CED-1C, amino acids 933 to 1111), and SNX-6 interacted with GST-CED-1N (Fig. 4F). No obvious interaction was detected between CED-1 and VPS-35 (Fig. 4F). Thus, CED-1 cycling is probably achieved by direct interaction with specific retromer subunits.

The retromer mediates a wide range of processes (*4*), including transport of intracellular sorting receptors such as Vps10 in yeast and CI-MPR (cation-independent mannose 6-phosphate receptor) in mammals (*13*, *14*), formation of Wnt gradients in *C. elegans* and *Drosophila* (*6*, *7*, *15*–*19*), and transcytosis of the polymeric immunoglobulin receptor in polarized epithelial cells (*20*). Retromer-mediated cycling of receptors is probably achieved by interaction of cargoes with different retromer subunits (*21*) or between cargoes and a retromer partner like Grd19/Snx3 (*22*). Our findings establish a function of retromer in apoptotic cell clearance in mediating cycling of the phagocytic receptor CED-1 between the plasma membrane and intracellular organelles. CED-1 family phagocytic receptors may be similarly regulated in other organisms.

References and Notes

1. P. W. Reddien, H. R. Horvitz, *Annu. Rev. Cell Dev. Biol.* **20**, 193 (2004).
2. R. S. Kamath, J. Ahringer, *Methods* **30**, 313 (2003).
3. P. J. Cullen, *Nat. Rev. Mol. Cell Biol.* **9**, 574 (2008).
4. J. S. Bonifacino, J. H. Hurley, *Curr. Opin. Cell Biol.* **20**, 427 (2008).
5. T. Wassmer *et al.*, *Dev. Cell* **17**, 110 (2009).
6. D. Y. Coudreuse, G. Roël, M. C. Betist, O. Destrée, H. C. Korswagen, *Science* **312**, 921 (2006).
7. B. C. Prasad, S. G. Clark, *Development* **133**, 1757 (2006).
8. E. A. Kritikou *et al.*, *Genes Dev.* **20**, 2279 (2006).
9. T. L. Gumienny, E. Lambie, E. Hartwieg, H. R. Horvitz, M. O. Hengartner, *Development* **126**, 1011 (1999).
10. X. Yu, S. Odera, C. H. Chuang, N. Lu, Z. Zhou, *Dev. Cell* **10**, 743 (2006).
11. Z. Zhou, E. Hartwieg, H. R. Horvitz, *Cell* **104**, 43 (2001).
12. A. Shi *et al.*, *EMBO J.* **28**, 3290 (2009).
13. C. N. Arighi, L. M. Hartnell, R. C. Aguilar, C. R. Haft, J. S. Bonifacino, *J. Cell Biol.* **165**, 123 (2004).
14. M. N. Seaman, J. M. McCaffery, S. D. Emr, *J. Cell Biol.* **142**, 665 (1998).
15. X. Franch-Marro *et al.*, *Nat. Cell Biol.* **10**, 170 (2008).
16. F. Port *et al.*, *Nat. Cell Biol.* **10**, 178 (2008).
17. T. Y. Belenkaya *et al.*, *Dev. Cell* **14**, 120 (2008).
18. C. L. Pan *et al.*, *Dev. Cell* **14**, 132 (2008).
19. P. T. Yang *et al.*, *Dev. Cell* **14**, 140 (2008).
20. M. Vergés *et al.*, *Nat. Cell Biol.* **6**, 763 (2004).
21. B. M. Collins, *Traffic* **9**, 1811 (2008).
22. T. I. Strochlic, T. G. Setty, A. Sitaram, C. G. Burd, *J. Cell Biol.* **177**, 115 (2007).

23. We thank S. Mitani, X. Wang, D. Xue, H. Fares, and *C. elegans* Genetic Center (CGC) for strains; X. Wang and H. Zhang for critically reading the manuscript; and I. Hanson for proofreading services. This research was supported by grants 2007CB947201, 30871266, and KSCX1-YW-R-70 from the Chinese government. C.Y. is supported by the Chinese Academy of Sciences 100-Talents Program.

Supporting Online Material

www.sciencemag.org/cgi/content/full/science.1184840/DC1
Materials and Methods
SOM Text
Figs. S1 to S12
Table S1
References

17 November 2009; accepted 22 January 2010
Published online 4 February 2010;
10.1126/science.1184840
Include this information when citing this paper.